

Transient Stability Assessment of Hybrid Distributed Generation and its Impact on Critical Clearing Time and Oscillation Duration Considering its Complementary Nature

P. K Olulope

Ekiti State University, Ado- Ekiti, Nigeria
paulade001@yahoo.com

Abstract— Presently, the grid accommodates several mixed energies so as to improve power generation and cater for demand which is ever increasing. These energy sources interact with each other and with the existing grid. Due to the complementary nature of most renewable energy and the mixed dynamics associated with them coupled with the bi directional power flow, transient stability based on single source will not give the overall assessment of the network. This paper presents the impact of hybrid Solar PV-Wind and Small Hydro distributed generation on transient stability of power system so as to take advantages of their complementary roles. To investigate this impact, a detail modeling of grid connected wind / solar PV and small hydropower system with single machine infinite system is carried out. The configuration of the proposed typical grid connected hybrid distributed generation (HDG) consists of hybrid Doubly fed induction generator (DFIG), solar PV and small hydropower system. DFIG is integrated through PWM converter into the existing grid while the solar PV consisting of DC sources is integrated through PWM inverter and the hydro power is directly connected through a synchronous generator. The simulation was done in DIgSILENT power factory software

Keywords— Hybrid distributed generation, stability index, and critical clearing time. Wind turbine, Solar PV, Hydropower system, export, import, distributed generation.

I. INTRODUCTION

The concept of distributed generation was introduced mainly to service loads locally and avoid excessive voltage drop due to long transmission. However, to meet most load demands locally the load must be shared among the locally integrated mixed energies for economic benefits. Besides, the energies are complementary which makes the assessment based on the combined energy sources important and relevant. In case of hybrid solar PV and

small hydro power, the solar PV supplies power only during the day and the small hydro power complement during the night [1]. This complementary roles and also the intermittency of the energy source need to be considered in order to give correct assessment of the system. The system dynamics is altered and more complexities are introduced when a hybrid sources are connected to distribution network compared to single energy sources. Hybrid distributed generation with multi-sources therefore can be defined as a small set of co-operating units that generates electricity and heat, with diversified primary energy carriers (Renewable and non-renewable), while the coordination of their operation takes place by utilization of advanced power electronics and are located close to the consumers end. They are either grid connected or standalone system, renewable or non-renewable system [2]. It can be described as distributed generation when it is connected close to the consumers to deliver power to local or industrial load [3]. There are many reasons why HDG is a focus for research. They are:

1. Since the DG complements one another, the outputs are also interdependent resulting in possibilities of higher degree of instabilities compare to single energy source.
2. Most renewable energies are weather dependent with constant daily load variation leading to negative impact on the entire system [6].
3. Economic load sharing among the distributed generators allow uneven participation of the generator and interaction with one another and the grid with tendency of higher degree of instability.
3. Possibilities of insufficient supply will be higher in a village with Solar PV alone or Solar PV combined with other renewable because PV does not supply energy during the nights.
4. Lack of inertia constant contributes to the poor voltage regulation and low power quality produce by PV array. It therefore increases instability during fault [8].

5. The existing control mechanism might not be able to handle load management, power interchange between the grid and the distribution network and the economic power supply
6. The renewable energies are stochastic in nature. So the output behavior solely depends on the environment. A robust transient stability models is needed
7. In the scheduling process, decisions to commit or de-commit units to meet the varying system load demand and the amount of spinning reserve required appropriate dynamic optimization programming which in a way contribute to different stability assessment output .

Today, most of the energy demand is supplied by conventional energy system such as fossil fuels which is characterized by greenhouse gases that can damage the environment and bring about serious health challenges. Our dependence on this is not advisable as the resources are not everlasting. In order to address these problems, renewable energies are introduced such as solar PV, Wind, Geothermal and hydropower system. Unfortunately most of these renewables are weather dependent and are mainly subject to variation. In some part of the world, the maximum availability of wind energy occurs during winter while solar energy peaks occurs in summer. On the other hand energy consumer requirements are highest during winter. These energy requirement might not be met by wind power alone, there is need to supplement with other renewable energies so as to benefits from their strength and thus reduce the effect of their weaknesses.

American wind energy association account for 1/5 of the global wind power available for US. Wind energy resources has characteristic of randomness, intermittent, unpredictable nature and cannot be stored which will result in instability of the grid. To solve this problem, there is need for good assessment of the system when three phase is applied as well as to employ the complementary capability of the wind, solar and small hydro power[1]. The complementary power is achieved when the generating system is combined in such away that the sufficiency of one energy is used to assist the deficiency of the other.

Due to this complimentary nature, there are wide-spread uses of hybrid distributed generation (hybrid Solar PV , Hydro power) across the globe though the level of penetration is still low [3, 4]. In 2011, few grid systems have penetration levels above five percent. Examples are Denmark – 26%, Portugal – 17%, Spain – 15%, Ireland – 14%, and Germany – 9%. For the U.S. in 2011, the penetration level was estimated at 2.9% [5].Germany, Demark and Ireland are already proposing a significant proportion of installed capacity to be connected to the distribution system below 100kV [6]. By year 2020, the

penetration level of DG in some countries such as USA is expected to increase by 25% as more independent power producers; consumers and utility company imbibe the idea of distributed generation [7]. In the same way, solar PV is gaining wide spread especially in Germany. 3% of total generation in Germany today is from solar PV. South Africa also concludes that the realization of the vision 2030 will be based on solar PV, Concentrated solar power (CSP) and wind power [8]. However, the rapid progress in renewable energy power generation technologies, and the awareness of environmental protection have been the major reasons why alternative energy and distributed generation is a promising areas [9].

The larger the penetration level of hybrid distributed generation (HDG) in a power system, the more difficult it becomes to predict, to model, to analyze and to control the behavior of such system [10]. Some HDG using induction generators are not grid friendly because they consume reactive power instead of generating it. Most power converters do not have adequate control mechanism to actively support DG integration. The system inertia for some of them (e.g., solar PV or fuel cell) is extremely low. They are weather dependent with constant daily load variation [11]. Also, existing protection mechanism might not be able to take care of the problem of bi-directional power flow that takes place due to DG connection in radial networks. New design controllers are needed to effectively manage the multi-energy sources distributed generation in other to service remote villages.

Due to the natural intermittent properties of wind and solar PV, stand alone wind/PV renewable energy systems normally require energy storage devices or some other generation sources to form a hybrid system.

In an electrical power grid without energy storage, energy sources that rely on energy stored within fuels (coal, oil, gas) must be scaled up and down to match the rise and fall of energy production from intermittent energy sources. In this way the operators can actively adapt energy.

II. DISTRIBUTED GENERATION AND HYBRID DISTRIBUTED GENERATION CONCEPT

Many of the primary energy sources are complimentary and abundant in nature which gives it a good opportunity to increase availability, power quality and flexibility of power supply when they are fully optimized. The objective of the integration is to capitalize on the strengths of both conventional and renewable energy sources, both cogeneration and non-cogeneration types. Presently, the promising sources of distributed generation are wind turbine and Solar PV. A PV cell harvest energy directly from sunlight and converting it to electricity. Due to the high cost, they were initially preferred only for space research applications. Later, as the cost of PV began to

decrease, several other applications were developed. Attempt to decrease the cost has brought the use of organic semiconductors like conjugated polymers [2] in the fabrication of solar cells. The locally made production of Solar panel is ongoing at least to reduce the high cost of production. However, the running cost and the maintenance cost of these PVs as well as the long life usage makes it an attractive alternative energy source. The drawbacks are:

- 1) The variability of the energy sources causes instability to the grid.
- 2) Consumers that are supplied by PV are likely to be in blackout in the night as PV does not supply energy during the nights.
- 3). Lack of inertia constant contributes to the poor voltage regulation and low power quality produce by PV array. It therefore increases instability during fault.

On the other hand, wind converts energy inherent in wind to electricity through wind turbine, shaft, induction generator and various controllers to ensure proper grid integration and friendliness. Like PV, wind output power depends on the availability of wind. The variability of energy sources is a concern as it is a hot area of research over decade ago. It is clean and renewable and environmentally friendly but is not reliable. Also, wind turbine especially the doubly-fed induction generator has the ability to provide supplementary active and reactive power to the existing grid.

For some reasons, solar PV and wind turbine can form a viable hybrid power sources. Other energy sources that can form hybrid sources with solar PV are diesel generator, batteries, fuel cells, small hydropower system. [2]. Detail of the list can be found in ref [2]. The location of wind and solar is site dependent and can be used in remote area where the cost of electricity is expensive

III. MODELING OF HYBRID DISTRIBUTED GENERATION

3.1 Modelling Doubly-Fed Induction Generator (DFIG) For Stability Studies

DFIG is widely preferred as the electrical generator for a wind turbine because of easy control and robustness [21]. DFIG is a wound rotor induction generator with voltage source converter connected to the slip-rings of the rotor. DFIG interact with the grid through the rotor and stator terminal. The induction generator is connected to the grid through the stator terminals, but the rotor terminals are connected to the grid via a partial-load variable frequency AC/DC/AC converter (VFC) [22] as shown in Fig. 1.

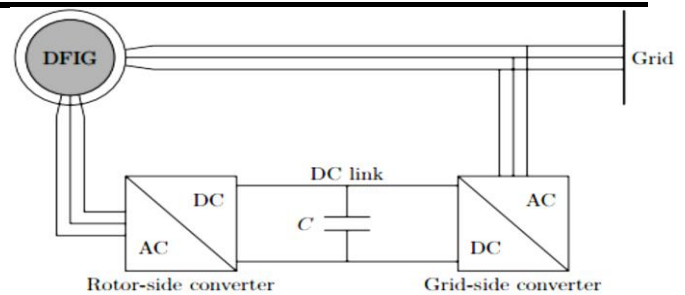


Fig. 1: DFIG with its converter [22]

To represent induction machine under system disturbance, it is desirable to use a double-cage model which represents transient and sub transient behaviour of the machine accurately [23-26]. For modelling the DFIG converters, it is assumed that the converters are ideal and the DC link voltage between the converters is constant. The rotor side converter is connected to the rotor of DFIG via brushes while the grid-side converter is connected to the grid. A capacitor is connected between the converters that act as DC voltage source. The DC voltage source decouples the rotor side converter from the grid-side converter. The rotor side converter is modelled as a voltage source whereas the grid-side converter is modelled as a current source [27],[28]. The torque and the speed are controlled by the rotor side converter. The rotor speed is controlled by q-component of the injected voltage, through rotor side converter. The d-component of the rotor side converter voltage is used for compensation for the generator magnetizing reactive power. The main objective for the grid-side converter is to keep the dc-link voltage constant. In DFIG, the rotor side converter is controlled by using different control techniques such as scalar and vector controls. In scalar control, the torque and flux have a coupling effect while in vector control, the torque and flux has a decoupling effect.

The DFIG equipped with four-quadrant ac-to-ac converter increases the transient stability margin of the electric grids compared to the fixed-speed wind systems based squirrel-cage generators [28]. The stator and the rotor modelling of DFIG are given below:

$$u_{ds} = -R_s i_{ds} - \omega_s \psi_{qs} + \frac{d\psi_{ds}}{dt} \quad (1)$$

$$u_{qs} = -R_s i_{qs} + \omega_s \psi_{ds} + \frac{d\psi_{qs}}{dt} \quad (2)$$

$$u_{dr} = -R_r i_{dr} - s\omega_s \psi_{qr} + \frac{d\psi_{dr}}{dt} \quad (3)$$

$$u_{qr} = -R_r i_{qr} + s\omega_s \psi_{dr} + \frac{d\psi_{qr}}{dt} \quad (4)$$

where s is the slip, u is the voltage, i is the current, R is the resistance, and ψ is the flux, is the synchronous speed of

the stator field. All quantities are measured in per unit. The subscripts d and q stand for direct and quadrature component, respectively while subscripts r and s stand for rotor and stator respectively.

The real and reactive power at the rotor and the stator can be calculated by:

$$P_s = u_{ds}i_{ds} + u_{qs}i_{qs} \quad (5)$$

$$Q_s = u_{qs}i_{ds} - u_{ds}i_{qs} \quad (6)$$

$$P_r = (u_{dr}i_{dr} + u_{qr}i_{qr}) \quad (7)$$

$$Q_r = (u_{qr}i_{dr} - u_{dr}i_{qr}) \quad (8)$$

For DFIG

$$P = P_s + P_r = u_{ds}i_{ds} + u_{qs}i_{qs} + u_{dr}i_{dr} + u_{qr}i_{qr} \quad (9)$$

$$Q = Q_s + Q_r = u_{qs}i_{ds} - u_{ds}i_{qs} + u_{qr}i_{dr} - u_{dr}i_{qr} \quad (10)$$

Rotor equations modeling

The general relations between wind speed and aerodynamic torque hold [17]:

$$T_t = \frac{1}{2} \rho \pi R^3 v^2 \frac{C_p(\lambda, \beta)}{\lambda} \quad (11)$$

And the power is shown as

$$P_w = \frac{\rho}{2} C_p(\lambda, \beta) A_R v_w^3 \quad (12)$$

The power coefficient C_p of the wind turbine in equation 12 is a function of tip-speed ratio λ which is given by:

$$\lambda = \frac{\omega R}{v} \quad (13)$$

T_t =turbine aerodynamic torque (Nm), ρ = specific density of air (kg/m³), v = wind speed (m/s), R =radius of the turbine blade (m), C_p = coefficient of power conversion, β = pitch angle, P =power extracted from the airflow (W), λ = Tip speed ratio,

ω = is the rotational speed of the wind turbine shaft

The value of Q fed into the grid in equation 11 above depends on the control of the power electronic in the grid sides. This does not affect active power except that the efficiency of the inverter can be incorporated into the last two variables. In this paper, for transient stability studies of power systems the generator is represented by third order model as indicated in DIGSILENT [21]. In this case the model is obtained by neglecting the stator transients for the fifth order model of induction machine. It shows that there are three electrical equations and one mechanical equation. The model is in d-q expressed in rotor reference frame. In rotor reference frame, the d axis in the rotor reference frame is chosen collinear to the rotor phase winding and the position of the rotor reference frame is the actual position of the rotor.

The dynamic model of the generator is completed by mechanical equation as indicated below:

The electrical torque can be expressed by:

$$T_e = \psi_{dr}i_{qr} - \psi_{qr}i_{dr} \quad (14)$$

Obviously, there is a change in generator speed as a result of the difference in electrical and mechanical torque. This is expressed as:

$$\frac{d\omega}{dt} = \frac{1}{2H} (T_m - T_e) \quad (15)$$

Where H is the inertial constant(s) and this is specified in DIGSILENT as acceleration time constant in the induction generator type. T_m and T_e is the mechanical and electrical torque respectively.

3.2 Modeling of Small Hydro Turbine

The power available in water current is proportional to the product of head and flow rate [30].

The general formula for any hydro power is:

$$P_{hyd} = \rho gQH \quad (16)$$

Where: P_{hyd} is the mechanical power produced at the turbine shaft (Watts), ρ is the density of water (1000 kg/m³), g is the acceleration due to gravity (9.81 m/s²), Q is the water flow rate passing through the turbine (m³/s), H is the effective pressure head of water across the turbine (m). The hydro-turbine converts the water pressure to mechanical shaft power, which further rotates the generator coupled on the same shaft [31-33]. The relation between the mechanical and the hydraulic powers can be obtained by using hydraulic turbine efficiency η_h , as expressed by the following equations:

$$P_n = \eta_h P_{hyd} \quad (17)$$

$$Q = Av$$

where A is the area of the cross section (m^2) and v is the water flow speed (m/s),

And the whole equation is derived from Bernoulli's theorem which states that:

$$\frac{v^2}{2g} + h + \frac{p}{\rho g} = \frac{P_{hyd}}{\rho g Q} \quad (18)$$

where p is the pressure of water (N/m^2).

3.3 Solar Cell Modeling

Solar PV effect is a basic physical process through which solar energy is converted directly into electrical energy. It consists of many cells connected in series and parallel. The voltage and current output is a nonlinear relationship. It is essential therefore to track the power since the maximum power output of the PV array varies with solar radiation or load current. The equivalent diagram of a solar cell is represented by one diode model as shown in Fig. 2.

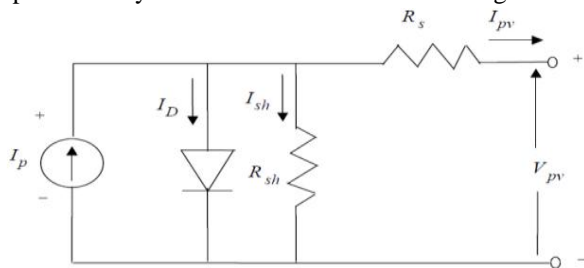


Fig.2: Model for single solar cell

The output terminal of the circuits is connected to the load. The output current source is the different between the photocurrent I_p and the normal diode current I_D . Ideally the relationship between the output voltage V_{pv} and the load current I_{pv} of a PV cell or a module can be expressed as if we assume that the current I_{sh} in shunt resistor R_{sh} is neglected. [33-36].

$$I_{pv} = I_p - I_D = I_p - I_o \left[\exp \left(\frac{V_{pv} + I_{pv} R_s}{m K T_c / q} \right) - 1 \right] \quad (19)$$

where I_p is the photocurrent of the PV cell (in amperes), I_o is the saturation current, I_{pv} is the load current (in amperes), V_{pv} is the PV output voltage (in volts), R_s is the series resistance of the PV cell (in ohms) and m , K and T_c

represent respectively the diode quality constant, Boltzmann's constant and temperature. q is electron charge (1.602×10^{-19} C) [38].

The power output of a solar cell is given by

$$P_{pv} = V_{pv} I_{pv} \quad (20)$$

Where I_{pv} is the output current of solar cell (A). V_{pv} is the solar cell operating voltage (V), P_{pv} is the output power of solar cell (W). The output power depends on the temperature and the irradiance [39].

IV. ARRANGEMENT OF THE PROPOSED CONFIGURATION

4.1 Modified Single Machine Infinite Bus System

Fig 3 shows the modified single machine infinite bus system model used in this paper. This power system model consists of an infinite bus system (Grid) represented by GEN1, one centralized generator (GEN2), a hybrid distributed generation (HDG) and two equal loads (LOAD1 and LOAD2). GEN1 is connected to bus 2 via line 3. The transmission lines (line 1, line2 and line3) are modeled as equivalent π transmission lines. Line 1 and line 2 are 100km long each, while line 3 is 40km long. GEN 2 is connected to bus 3 via a 100MVA transformer (transformer 1) and has a capacity of 80MW and 60MVar. The DG/HDG consisting of wind generator (DFIG), SOLAR PV and small hydropower system (SHP) is connected to bus 3 via another 100MVA transformer (Transformer 2). Each DFIG is rated 8MW, 0.89 power factor lagging. The SOLAR PV is rated 8MW real power at unity power factor. When SOLAR PV alone is connected to the HDG bus, a capacitor bank is used at that bus to compensate for reactive power. The hydropower is rated 8MW and 4MVar. LOAD1 and LOAD2 are connected to bus 2 and bus 3, respectively, and are rated 80MW and 40MVar each.

DIgSILENT power factor 14.1 was used to model this test system. To investigate the effect of a large disturbance, a three-phase fault was applied in the middle of line 2 and cleared after 200ms by removing the line.

Proposed Hybrid Distributed Generation Configuration

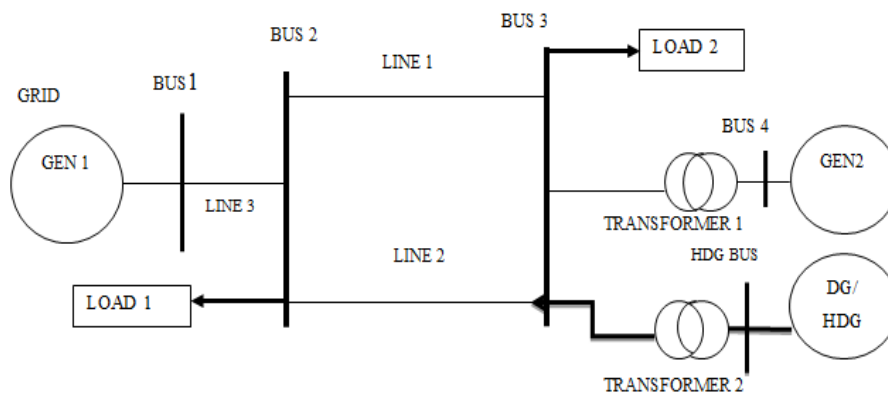


Fig.3: Modified Single Machine Infinite Bus System.

The focus is to investigate the impact of Hybrid solar PV, wind turbine (Doubly-Fed Induction Generator- DFIG) and small hydropower systems (SHP) on transient stability when it is used as complementary energy sources. In order to obtain all possible combinations, a truth table is formed as shown in Table 1. The truth table shows how the three generators can be combined to form HDG. The first column shows various scenarios. There are 8 scenarios.

For example, scenario 1 shows the case where there is no integration of DG/HDG. Scenario 2 shows the case where only SHP is integrated and so on. Zero (0) means no generator is connected while one (1) means a generator is connected. The base cases are single source DGs (Scenarios 2, 3 and 5). These base cases were chosen in order to draw out comparisons between complementary HDG and single source DG.

Table.1: Truth table describing the combination of different DG

SCENARIOS	WIND TURBINE (DFIG)	SOLAR PV	SMALL HYDROPOWER (SHP)	INFERENCE
1	0	0	0	No DG Integration
2	0	0	1	Small Hydropower only (Base case 1)
3	0	1	0	SOLAR PV only (Base case 2)
4	0	1	1	SOLAR PV and Small Hydropower
5	1	0	0	Wind turbine only (Base case 3)
6	1	0	1	DFIG and Small Hydropower
7	1	1	0	DFIG and SOLAR PV
8	1	1	1	DFIG, SOLAR PV, Small Hydropower (SHP)

PARTIAL ENERGY COMPLEMENTARITY INDEX

The partial energy complementarity index evaluates the relation between the average value of the availability functions. If the average values are equal the index should be equal to one (50% each). If those values are different the index should be smaller and tend to zero as the differences increase [42]

V. SIMULATION SCENARIOS

The simulation scenarios are discussed in this section. Case study 1 consists of scenarios 2 (Small Hydropower alone), 3 (SOLAR PV alone) and 5 (DFIG alone) which are the base cases. Case study 2 consists of scenario 4 (Hybrid SOLAR PV and Small Hydropower) Case study 3 consists of scenario 6 (Hybrid DFIG and Small Hydropower)

Case study 4 consists of scenario 7 (Hybrid DFIG and SOLAR PV)

Case study 5 consists of scenario 8 (Hybrid DFIG, SOLAR PV and Small hydropower)

Three penetration levels of HDG (PL_{HDG}) were considered:

- (i) Import mode, $PL_{HDG}=40\%$, %Complementarity ratio(CL_{HDG}): (50% equally)
- (ii) Balanced mode, $PL_{HDG}=50\%$, %Complementarity ratio(CL_{HDG}): (50% equally)
- (iii) Export mode, $PL_{HDG}=80\%$, %Complementarity ratio(CL_{HDG}): (50% equally)

The penetration level for HDG is defined as:

$$\% PL_{HDG} = \frac{P_{HDG}}{P_{HDG} + P_{CG}} \times 100 \quad (21)$$

where $\%PL_{HDG}$ is the percentage penetration of the DG/HDG, P_{HDG} is the active power generated by HDG and P_{CG} is the active power from the centralized generators (GRID and GEN2).

$$\%Complementarity\ level\ (CL_{HDG}) = \frac{P_{HDG}}{P_{LOAD}} \times 100 \quad (22)$$

Note that $P_{CG} + P_{HDG} = P_{LOAD}$

where P_{LOAD} is the power delivered to the load and $\%CL_{HDG}$ is the percentage complementarity level

In all the simulations, the active and the reactive power of GEN2 are kept constant. The descriptions of the penetration levels are as follows as well as complementary ratio:

Import mode: In this mode, the load demands are supplied by GEN2 and HDG with additional supply from the GRID. This is shown in Fig 4. The penetration level is 40% while the energy complementarity index is 50%

Balanced mode: In this mode, the load demands are met by the combination of GEN2 and HDG without any extra

supply from the GRID. This means that the power generated by HDG and GEN 2 is sufficient to meet the load demands. This is shown in Fig 5. The penetration level is 50% while the energy complementarity index is 50%

Export mode: In this mode, HDG and GEN2 supply the loads and export the excess generation to the GRID. This is shown in Fig 6. The penetration level is 80% while the energy complementarity index is 50%

VI. TRANSIENT STABILITY INDICATOR

6.1 Impact of Hybrid Distributed Generation Using CCT

To measure the impact of HDG on transient stability, the critical clearing time (CCT) is used as the stability index. This index measures the stability margin and indicates the robustness of the system to disturbances. The longer the CCT, the longer the system can tolerate the fault, and the more robust is the system. The impact of penetration level and based on import mode, balanced mode and export mode on transient stability with HDG is investigated by monitoring the CCT. To assess the level of instability, the rotor angle is monitored when a temporary three-phase fault is applied in the middle of line 2 while the CCT is monitored by applying three-phase fault on line 2 at different locations from bus 3. The locations of the fault are 0%, 20%, 40%, 60%, 80% 100% of the total length of the transmission line (bus 3-bus2). In other word, the fault distance is the distance from bus 3 to the fault location. For example, when the fault occurs at bus 3, the fault location will be 0% and when the fault occurs at bus 2, the fault location will be 100% and so on. The CCT is calculated by increasing the fault clearing time (FCT) until the rotor angle of GEN 2 reaches its critical clearing angle where further increase will make the system unstable.

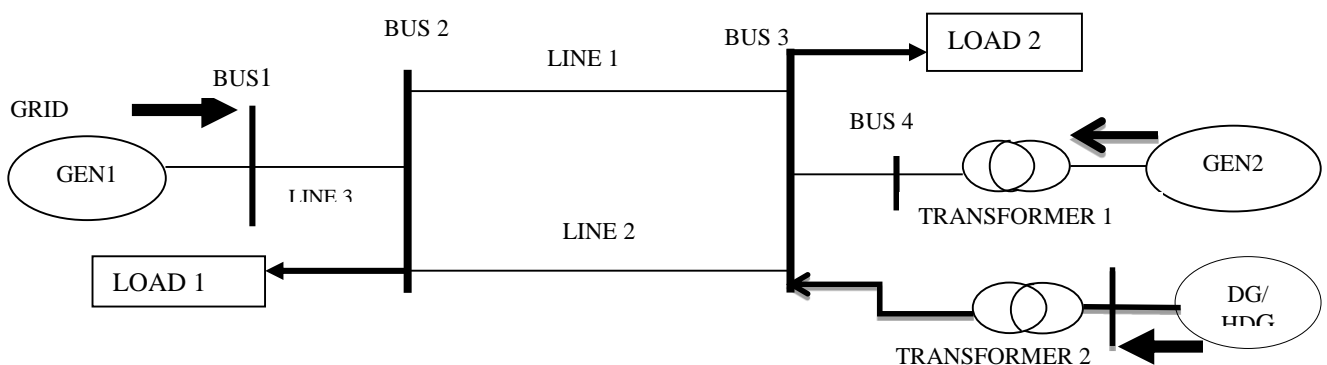


Fig.4: Modelling configuration for import mode

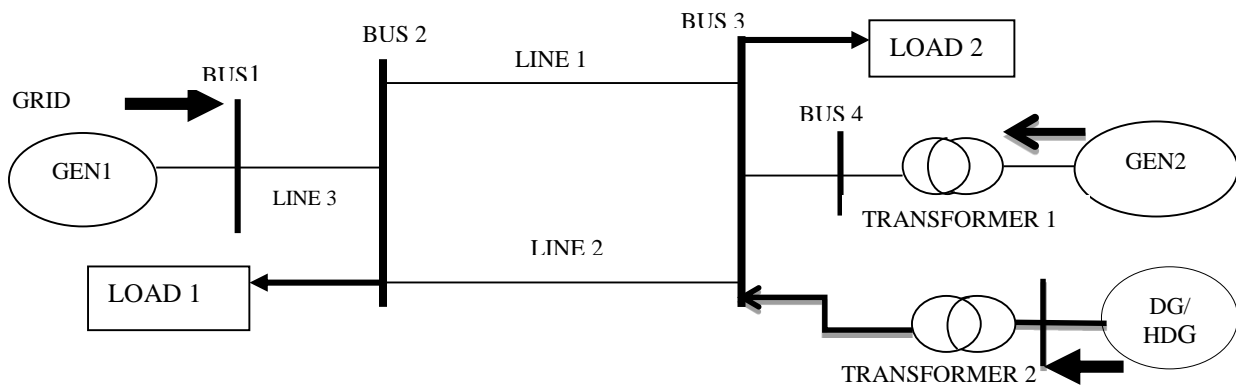


Fig.5: Modeling configuration for balanced mode

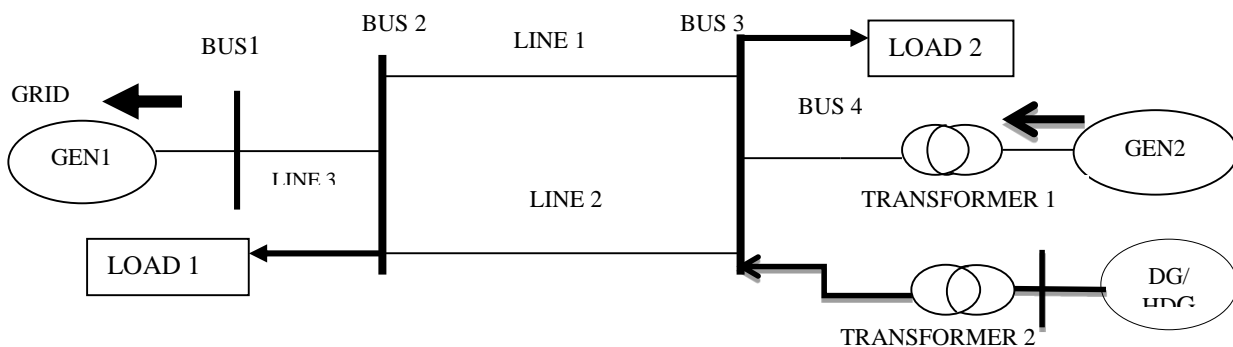


Fig.6: Modeling configuration for export mode

VII. TRANSIENT STABILITY SIMULATION RESULTS

For the simulation results in this section, the following factors have been taken into consideration: Penetration level, HDG type and location of HDG in order to explain the behavior when it is complementary.

7.1 HDG Penetration Level and Different HDG Impact on Rotor Angle

The graphs in Figs 7-9 show the rotor angle swings of GEN 2 when SOLAR PV alone, DFIG alone and HYBRID DFIG +SOLAR PV are integrated into the system. The import mode, balanced mode and export mode are shown in Fig 7, Fig 8 and Fig 9, respectively. From Fig 7, it can be observed that when DFIG alone was integrated into the system, the first swing of GEN 2 rotor angle is the highest (i.e., -4.99°) compared to when SOLAR PV and HYBRID DFIG+SOLAR PV were integrated. The second highest first swing occurs with HYBRID DFIG +SOLAR PV, (i.e., -8.36°). The smallest first swing is shown when SOLAR PV alone is connected (i.e., -15.13°). It can be seen that when DFIG alone was connected the system has more oscillations compared with the cases with SOLAR PV alone and HYBRID DFIG+SOLAR PV. This suggests that when DFIG alone is integrated into the system, the system is prone to more instability compared to SOLAR

PV alone and HYBRID DFIG+SOLAR PV. This is due to the crowbar which is triggered to block the rotor side converter and as a result, the voltage cannot recover completely immediately after the fault is cleared because the rotor side converter cannot provide the necessary reactive power to the generator for magnetization purpose. The generator then absorbs reactive power from the grid. When HYBRID DFIG+SOLAR PV is connected, the system is more transiently stable than when DFIG alone is connected. This can be seen at the settling time. The settling time when HYBRID DFIG+SOLAR PV is integrated into the grid is 8 seconds compared with 10 seconds for DFIG alone. The combination of DFIG and SOLAR PV has improved the first swing and the subsequent swings. This is because of the good transient stability characteristics of SOLAR PV. When SOLAR PV alone is used, the system seems to have a better transient stability in terms of first swing compared with when HYBRID DFIG+SOLAR PV is used. However, for the subsequent oscillations, when SOLAR PV alone or when HYBRID DFIG+SOLAR PV is used, they have similar settling time. The same explanations can be applied to the balanced mode in Fig 8 and export mode in Fig 9. However, at the export mode, the GEN 2 rotor angle went out of step when DFIG alone was connected. This is

because the penetration of DFIG is now high (80%). The HYBRID DFIG+SOLAR PV and SOLAR PV are transiently stable as shown in Fig 9 compared to when

DFIG alone is used. The settling time when HYBRID DFIG+SOLAR PV is used is faster than when SOLAR PV alone or DFIG alone are used.

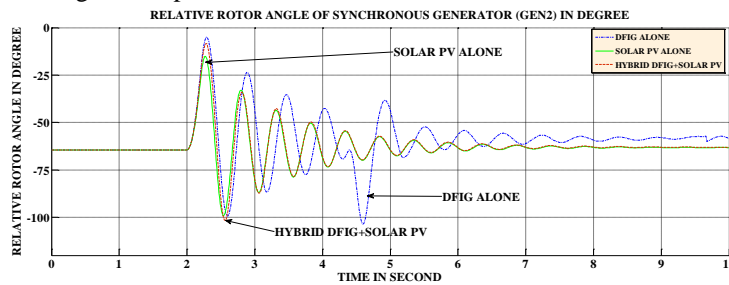


Fig.7: Comparison of the impact of SOLAR PV alone, DFIG alone and HYBRID DFIG+SOLAR PV on the rotor angle of GEN2 (Import mode)

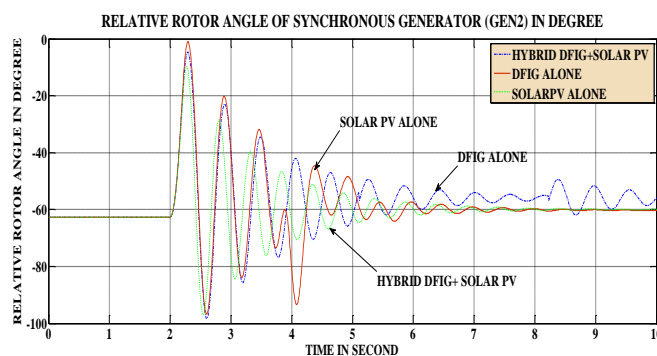


Fig.8:Comparison of the impact of SOLAR PV alone, DFIG alone and HYBRID DFIG +SOLAR PV on the rotor angle of GEN2 (Balanced mode)

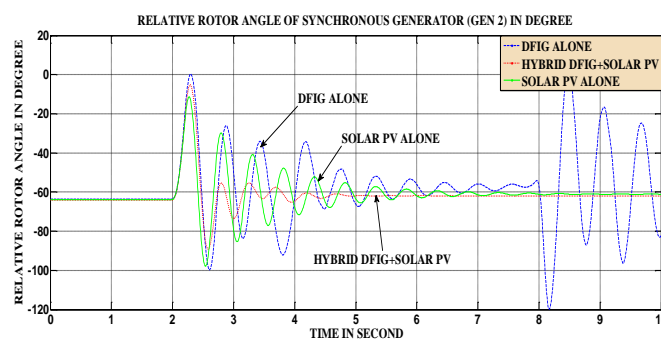


Fig 9: Comparison of the impact SOLAR PV alone, DFIG alone and HYBRID DFIG +SOLAR PV on the rotor angle of GEN2 (Export mode)

As it can be seen, the instability increases as the penetration level of the DG/HDG increases. If HYBRID DFIG+SOALR PV is used, the rotor angle shows a reduced first swing compared to DFIG alone.

Figs 10-12 show the simulation results when HYBRID DFIG+SOLAR PV, HYBRID DFIG+SHP, HYBRID SOLAR PV+SHP and DFIG alone were integrated into the grid, for import, balanced and export modes respectively. For import mode, (see Fig 10), there is not much difference in the first swing of rotor angle of all the curves though the highest first swing occurs when DFIG alone is integrated. The same happened in Fig 11, the rotor angle of GEN 2 when DFIG alone was integrated shows the highest instability. HYBRID SOLAR PV+SHP shows improved

stability compared to DFIG alone. For the export mode (see Fig 12), the rotor angle of GEN2 when DFIG alone was integrated went out of step but when DFIG alone was combined with other energy sources (HYBRID DFIG+SOLAR PV, HYBRID DFIG+SHP), the transient stability is improved. When HYBRID SOLAR PV+SHP was used, the rotor angle of GEN 2 is more stable compared to the rest in Fig 12. The three hybrids (HYBRID DFIG+SOLAR PV, HYBRID DFIG+SHP, HYBRID SOLAR PV+SHP) settle down within 6 seconds while the DFIG alone is unstable even up till 10 seconds. HYBRID SOLAR PV+SHP shows the lowest first swing, followed by HYBRID DFIG+SHP, and then HYBRID DFIG+SOLAR PV.

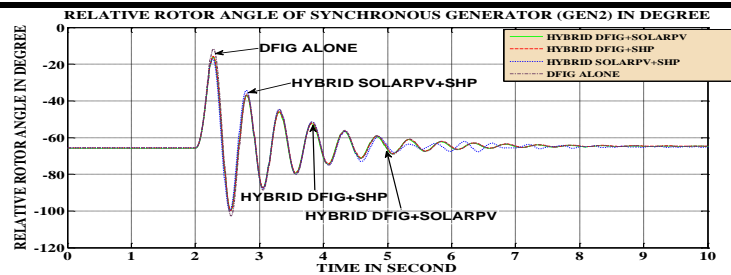


Fig.10: Comparison of the impact of HYBRID DFIG+ SOLAR PV, HYBRID DFIG+ SHP, HYBRID SOLAR PV +SHP, and DFIG alone system on the rotor angle of GEN2 (Import mode)

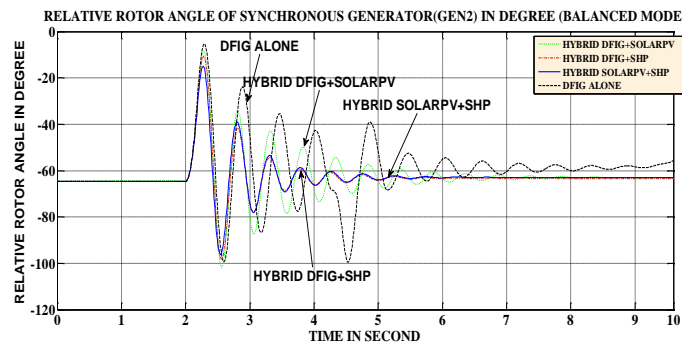


Fig.11: Comparison of the impact of HYBRID DFIG+ SOLAR PV, HYBRID DFIG+ SHP, HYBRID SOLAR PV +SHP, and DFIG alone system on the rotor angle of GEN2 (Balanced mode)

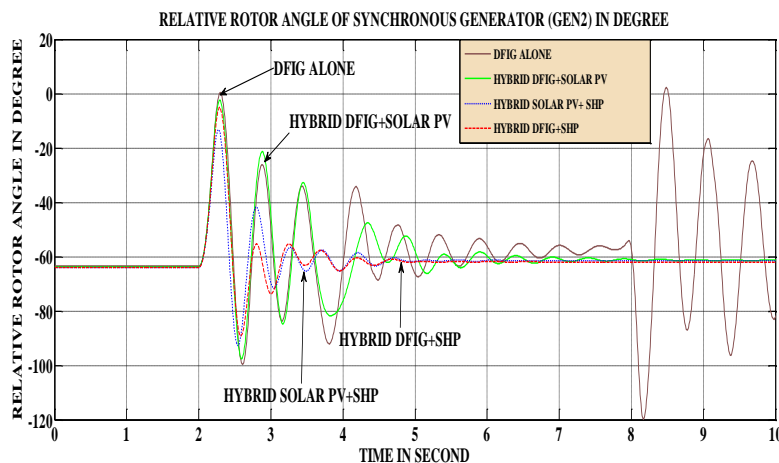


Fig.12: Comparison Of the impact of HYBRID DFIG+ SOLAR PV, HYBRID DFIG+ SHP, HYBRID SOLAR PV +SHP, and DFIG alone system on the rotor angle of GEN2 (Export mode).

It is already established from the simulations in Figs 7-12 that as the penetration level increases the instability also increases irrespective of the HDG type used. As a result of this, export mode

7.2 HDG Penetration Level and Different Fault Locations Impact on Critical Clearing Time (CCT)

In this section, the impact of HDG penetration level, different HDG types and fault locations on the critical clearing time (CCT) is investigated. The decrease in critical clearing time (CCT) indicates an increase in instability (decrease stability margin). Tables 2-4 show the CCT values and the average values of the CCT of the power system network for import, balanced and export modes when SHP alone, SOLAR PV alone and DFIG

alone were integrated into the system, respectively. From Tables 2-3, it is observed that, as the fault location is increasing from 0% to 60%, the CCT values also increased from relatively smaller values to maximum values and then decreased again from 80% fault location to 100%. This is fairly in agreement with the literature which state that the maximum transfer admittance occurs at the midpoint of the transmission line. The curve between transfer admittance and the distance of the fault will be symmetrical about 0.5 p.u. length, where maximum transfer admittance occurs if the circuit is symmetrical about the middle of the line. The CCT value will begin to decrease after the midpoint. Table 4 followed a similar pattern except for export mode where the maximum value

of the CCT occurs at location 80% instead of 60%. However, the difference between the maximum CCT value of 80% and that at 60% is marginal (i.e., 0.0185%) which can be neglected.

Also from Tables 2-4, it can be seen that the transient stability margin decreases with increasing penetration level. For example, in Table 2, when the fault was applied at 100km from bus 3, i.e. exactly on bus 2, the CCT value decreases from 280ms in the import mode to 278ms in the balanced mode and later to 270ms in the export mode. The average value of the CCT at the import mode is 333.3ms, balanced mode is 329.7ms and the export mode is 318.5ms. This shows that, as the penetration level of the HDG increases, the CCT decreases (i.e., transient stability margin reduces). The same applied to Tables 3-4. As the penetration level increases, the decrease in the CCT values is very significant when DFIG alone is used compared to other DGs. This can be explained why the system with DFIG became unstable at export mode. This can be seen from the average values of the CCT reported in Tables 2-4. Furthermore, the CCT value depends on the type of DG used. For example, the average values of the CCT when SHP alone is integrated into the grid (see Table 2) are higher at all the modes than the average values of the CCT when SOLAR PV alone is integrated into the grid (see Table 3). The average values of the CCT at all the modes when DFIG alone is connected to the grid are the smallest. This suggests that instabilities arising from integrating DFIG alone are higher compared to when SOLAR PV alone and SHP alone are connected. These CCT values agreed with the initial simulations when the rotor angle was monitored that the increase in penetration level increases the transient instability.

Table.2: The critical clearing time of synchronous generator (GEN2) with integrated SHP Alone

SHP Alone			
Fault location	Import mode	Balanced mode	Export mode
%	CCT (ms)	CCT (ms)	CCT (ms)
0	280	267	256
20	320	315	310
40	370	370	356
60	390	390	370
80	360	355	349
100	280	278	270
Average (ms)			
	333.3	329.7	318.5

Table.3: The critical clearing time of synchronous generator (GEN2) with integrated SOLAR PV Alone

SOLAR PV Alone			
Fault location	Import mode	Balanced mode	Export mode
%	CCT (ms)	CCT (ms)	CCT (ms)
0	265	260	255
20	310	300	295
40	350	340	330
60	370	350	340
80	340	320	310
100	265	250	240
Average (ms)			
	316.7	303.3	295

Table.4: The critical clearing time of synchronous generator (GEN2) with integrated DFIG Alone

DFIG Alone			
Fault location	Import mode	Balanced mode	Export mode
%	CCT (ms)	CCT (ms)	CCT (ms)
0	250	40	30
20	290	60	40
40	320	70	50
60	330	80	53
80	310	70	54
100	240	90	40
Average (ms)			
	290	68.3	44.5

Tables 5–7 show the CCT values and the average values of the CCT when HYBRID SOLAR PV+SHP, HYBRID DFIG+SHP and HYBRID DFIG+SOLAR PV were integrated into the grid, respectively.

For example, at the export mode, the average values of the CCT for HYBRID SOLAR PV+SHP, HYBRID DFIG+SHP and HYBRID DFIG+SOLAR PV are 290ms, 256.7ms and 216.7ms, respectively.

This suggests that when HYBRID SOLAR PV+SHP is used, the system is more transiently stable (improved stability margin) compared to when HYBRID DFIG+SHP and HYBRID DFIG+SOLAR PV were used. This can be seen also from all the modes in Tables 5-7.

Comparing hybrid type with a single source, the average values of the CCT when HYBRID SOLAR PV+SHP is used indicates an improved stability compared to when DFIG alone and SOLAR PV alone are used except in the export mode of SOLAR PV. But in the case of SHP alone, the average values of the CCT are higher at the balanced and export modes alone compared to when HYBRID SOLAR PV+SHP is used.

The CCT values and the average values of the CCT when HYBRID DFIG+SOLAR PV+SHP is connected to the grid are shown in Table 8. It can be seen that for the export mode, the average value of the CCT is smaller compared to other hybrids in Tables 5-7. The average values of the CCT for the import and the balanced modes in Fig 8 are generally smaller than the hybrid with two DGs such as HYBRID SOLAR PV +SHP and HYBRID DFIG+SHP except in the balanced mode when HYBRID DFIG+SHP is used. The difference between the average value of the CCT at a balanced mode when HYBRID DFIG+SOLAR PV+SHP and HYBRID DFIG+SHP is used is small (i.e., 0.0181%) and can be neglected. However, the average values of the CCT for HYBRID DFIG+SOLAR PV+SHP are higher at the import and balanced mode compared with when HYBRID DFIG+SOLAR PV is used. This suggests that the system with three DGs is more prone to instability than the system with two DGs and the stability worsen as the penetration increases compared to other hybrids.

Table.5: The critical clearing time of synchronous generator (GEN2) with integrated HYBRID SOLAR PV+SHP

HYBRID SOLAR PV+SHP			
Fault location	Import mode	Balanced mode	Export mode
In %	CCT(ms)	CCT(ms)	CCT(ms)
0	270	267	260
20	330	310	300
40	390	360	320
60	420	370	330
80	390	340	300
100	290	260	230
Average (ms)			
	348.3	317.8	290

Table.6: The critical clearing time of synchronous generator (GEN2) with integrated HYBRID DFIG+SHP

HYBRID DFIG+SHP			
Fault location	Import mode	Balanced mode	Export mode
In%	CCT(ms)	CCT(ms)	CCT(ms)
0	250	240	200
20	303	300	270
40	350	330	290
60	380	350	290
80	350	320	270
100	255	250	220
Average (ms)			
	326.6	298.3	256.7

Table.7: The critical clearing time of synchronous generator (GEN2) with HYBRID DFIG +SOLAR PV

HYBRID DFIG +SOLAR PV			
Fault location	Import mode	Balanced mode	Export mode
In %	CCT(ms)	CCT(ms)	CCT(ms)
0	240	250	150
20	295	290	230
40	340	310	210
60	360	320	230
80	330	290	260
100	240	240	220
Average (ms)			
	300.8	283.3	216.7

Table 8: The critical clearing time of synchronous generator with integrated HYBRID DFIG+SOLAR PV+SHP

HYBRID DFIG+SOLAR PV+ SHP			
Fault location	Import mode	Balanced mode	Export mode
In %	CCT(ms)	CCT(ms)	CCT(ms)
0	256	252	100
20	300	300	160
40	340	340	210
60	360	360	240
80	310	330	220
100	250	240	150
Average (ms)			
	302.7	303.7	180

Comparing the export mode of Table 7 and Table 8, it shows that from a stability point of view and based on the simulation results, the stability is improved when DFIG is hybridized with other DG but worsen when hybridized with two DGs under a high penetration level. At import mode and balanced mode when the penetration is low and moderate, respectively, the average values of the CCT when HYBRID DFIG+SOLAR PV+SHP is used is better than when HYBRID DFIG+SOLAR PV is used. However, the average CCT when HYBRID DFIG+SOLAR PV+SHP is used is lower compared to when HYBRID SOLAR PV+SHP was used at all the modes.

The CCT value depends on the penetration level, fault location as well as the HDG types used. The CCT decreases with increase in penetration level irrespective of the HDG types used.

7.3 HDG Penetration Level and Location of HDG Impact on Rotor Angle

The location of HDG is determined by the availability of primary energy source. HDG should be sited in a place

where the primary energy source is abundantly available. HDG can be sited at a single point (concentrated) or on several places in such a way that the generators are centrally coordinated (dispersed). Dispersed HDG is assumed to be close to the load (e.g., rooftop solar PV) while concentrated is located where the energy source could be found and possibly far from the load. This section explains the impact of HDG on the grid when the HDGs are dispersed, and when they are concentrated on a single point. Note that the simulation results presented in this section are for export mode only. The followings were investigated:

- 1) Dispersed and concentrated HYBRID SOLAR PV + SHP
- 2) Dispersed and concentrated HYBRID DFIG+ SHP

- 3) Dispersed and concentrated HYBRID DFIG+ SOLAR PV

7.4 Location of HDG Impact on Rotor Angle

Fig 13-Fig 15 shows the simulations that are used to investigate the impact of the location of HDG on transient stability. It is observed from the simulations that transient stability margin is improved (i.e., smaller first swing and quicker settling time) when dispersed HDG is used compared to concentrated HDG. The reason for this is probably due to the higher voltage drop in the concentrated compared to dispersed HDG since dispersed HDG is generally close to the load, therefore the voltage drop is small.

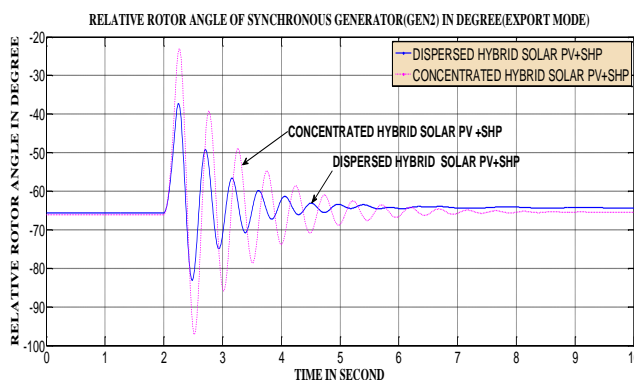


Fig 13: Rotor angle of GEN2 with concentrated and dispersed HYBRID SOLAR PV+ SHP

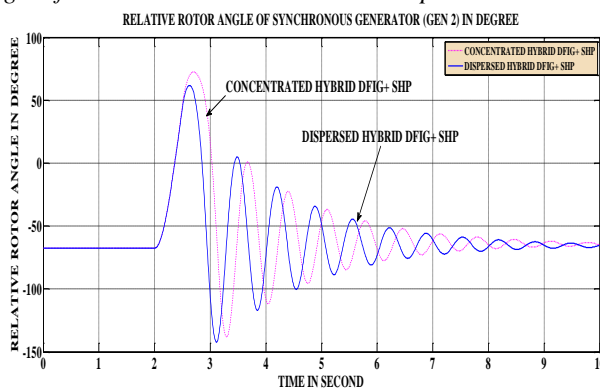


Fig14: Rotor angle of GEN2 with concentrated and dispersed HYBRID DFIG+ SHP

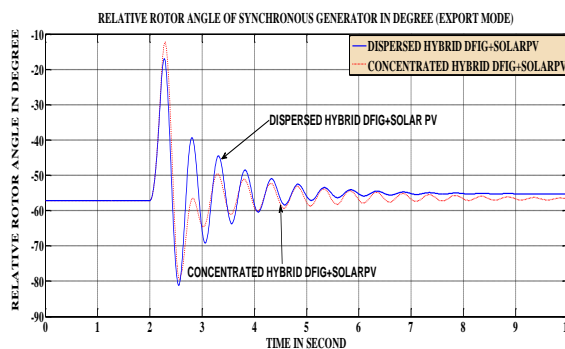


Fig 15: Rotor angle of GEN2 with concentrated and dispersed HYBRID DFIG+ SOLAR PV

In all the graphs (Fig 13-Fig 15), concentrated HDG shows higher first swing and longer settling time compared to dispersed HDG. It can also be seen that the impact of transient stability depends on the HDG type involved. For example, HDG using SOLAR PV and SHP is more stable than HYBRID DFIG+SHP or HYBRID DFIG+SOLAR PV. The less stable system is hybrid DFIG+SOLAR PV.

7.5 Location of HDG Impact on Critical Clearing Time (CCT)

Again, in this section, only the results of export mode are shown. The CCTs for concentrated and dispersed HDG systems at export mode are shown in Table 9. For example, when HYBRID SOLAR PV+SHP is used, the CCT when dispersed HDG is used is 375ms compared to 330ms for concentrated HDG. The remaining values in the table also show that dispersed HDG has an improved stability compared to concentrated HDG. This further supports the results already established in the above simulations that the transient stability of a dispersed generation is better than concentrated HDG.

Table 9: Critical clearing time of a synchronous generator (GEN2) for concentrated and dispersed HDG scenarios

	CCT (ms) (Dispersed)	CCT (ms) (Concentrated)
HYBRID SOLAR PV + SHP	375	330
HYBRID DFIG+ SHP	380	265
HYBRID DFIG+ SOLAR PV	310	300
HYBRID DFIG+SOLAR PV+ SHP	250	230

VIII. CONCLUSION

When HDG is employed in distributed generation concept for voltage control and load balancing, it is transiently stable compare to when single source DG is employed. Generally, it is accepted that most DG are complementary but it might not be transiently stable. The results in this paper show that DFIG with other energy sources shows increasing instability even as the penetration level increases. Transient stability under complementarity nature depends on the HDG types, penetration level and the location of the DG.

REFERENCES

[1] F.Monforti et al ‘ Assessing complementarity of wind and solar resources for energy production in Italy. A Monte Carlo approach. Renewable Energy 63 (2014) pp576-586.

[2] T.Ackerman,G. Andersson, and L.Soder. “Distributed generation, a definition” Electric Power Energy Research Vol,57, no3, pp195-204, 2001

[3] J.Momoh, G.D.Boswell, “Improving power Grid Efficiency using Distributed Generation” Proceedings of the 7th international conference on power system operation and planning, pp.11-17, Jan., 2007.

[4] <http://www.energy.ca.gov/2007publications/CEC-500-2007-021/CEC-500-2007-021.PDF>.

[5] A.M.Azmy, “ Simulation and Management of Distributed Generation units using intelligent techniques”, Ph.D. Thesis submitted to the department electrical engineering University of Duisburg-Essen 2005.

[6] P.K Olulope, K.A Folly, “Impact of Hybrid Distributed Generation On Transient Stability of Power System” Power and Energy Systems Applications (PESA 2012), Las Vegas, USA, November 12 – 14, 2012, pp97-105.

[7] P.K Olulope, K.A Folly, Ganesh K. Venayagamoorthy, “Modeling And Simulation of Hybrid Distributed Generation and Its Impact on Transient Stability of Power System”, International conference on Industrial technology (ICIT) 2013, 25-27 February 2013.

[8] J Paska, P.Biczal, M.Klos, “Hybrid power systems- An effective way of utilizing primary energy sources”, Electric Power Systems Research, Elsevier, 2009, pp.1-8.

[9] C. Wang, “Modeling and control of hybrid Wind/photovoltaic/fuel cell distributed generation system”.Ph.D Dissertation submitted to Montana State University, July 2006.

[10] V.V Thong, J. Driesen, R. Belmans, “Transmission system operation concerns with high penetration level of distributed generation”, Universities power and Engineering Conference UPEC, pp.867-8717, 4-6Sept., 2007.

[11] T. Tran-Quoc, L.Le Thanh, Ch.Andrieu, N. Hadjsaid, C. Kieny, J.C Sabonnadiere, K. Le, O. Devaux, O.Chilard “Stability analysis for the distribution networks with distributed generation” Proc.2005/2006 IEEE/PES Transmission & Distribution Conference & Exposition, vol. 1–3, Dallas, TX, USA, May 21–26 pp. 289–294. 2006.

[12] V.V. Knazkins “Stability of Power Systems with Large Amounts of Distributed Generation” PhD Thesis submitted to University Stockholm, Sweden, 2004.

[13] A Ishchenko “Dynamics and stability of distributed networks with dispersed Generation”, Ph.D thesis

- submitted to Eindhoven University of technology, 16 Jan., 2008.
- [14] M. Reza, "Stability analysis of transmissions Systems with high penetration of distributed generation", PhD Thesis submitted to Delf University of Technology Delft, The Netherlands, 2006.
- [15] Y. Tiam, "Impact on the power system with a large generation of photovoltaic generation", PhD Thesis submitted to the University of Manchester Institute of Science and Technology, Feb., 2004, pp.53-55.
- [16] Vechiu I, Camblong H, Papiu G, Dakyo B, Nichita C. Dynamic simulation model of a hybrid power system: performance analysis. International Journal of Automotive Technology 2006;7(7):1-9.
- [17] S. Sotirios B, Papadopoulos P. Demetrios. "Efficient design and simulation of an expandable hybrid (wind-photovoltaic) power system with MPPT and inverter input voltage regulation features in compliance with electric grid requirements. Electric Power Systems Research 2009;79:1271-85
- [18] Mehdi Dali, Jamel Belhadj, Xavier Roboam. Design of a stand-alone hybrid photovoltaic-wind generating system with battery storage, http://journal.esrgroups.org/jes/papers/4_3_7.pdf.
- [19] Joanne Hui, Alireza Bakhshai, Praveen K. Jain. A hybrid wind- solar energy system: a new rectifier stage topology. In: Applied Power Electronics Conference and Exposition (APEC), 2010 Twenty-Fifth Annual IEEE, 21e25 Feb., 2010, pp. 155-61.
- [20] Arutchelvi Meenakshisundaram, Daniel Samuel Arul. "Grid connected hybrid dispersed power generators based on PV array and wind-driven induction generator". Journal of Electrical Engineering 2009;60(6):313-20.
- [21] A. D. Hansen, C. Jauch, P. Sørensen, F. Iov, F. Blaabjerg, "Dynamic wind turbine models in power system simulation tool DIGSILENT", Rsis National Laboratory, Roskilde, Dec. 2003. Access: www.digsilent.es/tl_files/digsilent/files/powerfactory/application.../ris-r-1400.pdf
- [22] L. L. Freris, *Wind energy conversion systems*. Prentice Hall, 1990.
- [23] P. E. Sørensen, A.D. Hansen, L. Janosi, J. Bech, and B. Bak-Jensen, "Simulation of Interaction between Wind Farm and Power System." Technical University of Denmark Dec-2002. Access: orbit.dtu.dk
- [24] M. V. A. Nunes, J. A. P. Lopes, H. H. Zurn, U. H. Bezerra, and R. G. Almeida, "Influence of the variable-speed wind generators in transient stability margin of the conventional generators integrated in electrical grids," *IEEE Trans. Energy Convers.*, vol. 19, no. 4, pp. 692 – 701, Dec. 2004.
- [25] J. Morren and S. W. H. de Haan, "Ridethrough of wind turbines with doubly-fed induction generator during a voltage dip," *IEEE Trans. Energy Convers.*, vol. 20, no. 2, pp. 435 – 441, Jun. 2005.
- [26] J. B. Ekanayake, L. Holdsworth, X. Wu, and N. Jenkins, "Dynamic modeling of doubly fed induction generator wind turbines," *IEEE Trans. Power Syst.*, vol. 18, no. 2, pp. 803 – 809, May 2003.
- [27] M. A. Poller, "Doubly-fed induction machine models for stability, assessment of wind farms," in *Power Tech Conference Proceedings 2003 IEEE Bologna*, 2003, vol. 3, p. 6 pp. Vol.3.
- [28] W. Qiao, "Dynamic modeling and control of doubly fed induction generators driven by wind turbines," in *Power Systems Conference and Exposition, 2009. PSCE '09. IEEE/PES*, 2009, pp. 1 –8.
- [29] D. Gautam, V. Vittal, and T. Harbour, "Impact of increased penetration of DFIG based wind turbine generators on transient and small signal stability of power systems," in *2010 IEEE Power and Energy Society General Meeting*, 2010, p. 1.
- [30] Dolf Gielen, "Renewable Energy Technologies; Cost Analysis Series." IRENA International Renewable Energy Agency, Jun- 2012.
- [31] H. Ramos, "Guidelines For Design of Small Hydropower Plants." Jul-1999.
- [32] "Small Hydropower Systems," U.S. Department of Energy (DOE) by the National Renewable Energy Laboratory (NREL), Jul. 2001.
- [33] Hydropower basics <http://www.microhydropower.net/basics/turbines.php>.
- [34] L. Ye, H. B. Sun, X. R. Song, and L. C. Li, "Dynamic modeling of a hybrid wind/solar/hydro microgrid in EMTP/ATP," *Renew. Energy*, vol. 39, no. 1, pp. 96–106, Mar. 2012.
- [35] Mukund R. Patel, Ph.D., P.E., *Wind and Solar Power Systems*. United States of America: CRC Press.
- [36] L. Gray,, *The physics of the solar cell A. Luque, S. Hegedus (Eds.), Handbook of Photovoltaic Science and Engineering, Wiley, New York (2003), pp. 61–111 (Chapter 3)*.
- [37] R. Chenni, M. Makhlof, T. Kerbache, and A. Bouzid, "A detailed modeling method for photovoltaic cells," *Energy*, vol. 32, no. 9, pp. 1724–1730, Sep. 2007.
- [38] Ramos Hernanz et.al, "Modelling of Photovoltaic Module", International Conference on Renewable Energies and Power Quality ICREPQ'10) Granada (Spain), 23th to 25th March, 2010..
- [39] M.de Blas, J. Torres, E. Prieto, and A.Garcia, "Selecting a suitable model for characterizing

- photovoltaic devices,” *Renew. Energy*, vol. 25,no.3, pp. 371–380, Mar. 2002
- [40] J. Kepka, ‘Load Modeling for Power System Analysis” Poland: Wroclaw University of Technology; 2014. p. 1–4. Access: eeeic.org/proc/papers/111.pdf
- [41] P.K Olulope, ‘Transient Stability Assessment of Hybrid Distributed Generation Using Computational Intelligence Approaches’ PhD Thesis submitted to University of Cape Town Department of Electrical Engineering, South Africa, June, 2014. Solar plants to provide
- [42] A. Beluco et al ‘Dimensionless index evaluating the time complementarity between solar and hydraulic energies’ *Renewable Energy* 33 (2008) 2157-2165